Materials Science in Semiconductor Processing 56 (2016) 394–402

Contents lists available at ScienceDirect

Materials Science in Semiconductor Processing

journal homepage: www.elsevier.com/locate/mssp

Effect of particle size on optical and electrical properties in mixed CdS and NiS nanoparticles synthesis by ultrasonic wave irradiation method

V. Mohanraj[a], R. Jayaprakash[a,*], R. Robert[b], J. Balavijayalakshmi[c], S. Gopi[a]

[a] Nanotechnology Laboratory, Department of Physics, Sri Ramakrishna Mission Vidyalaya College of Arts and Science, Coimbatore 641020, Tamil Nadu, India
[b] Department of Physics, Government Arts College (Men), Krishnagiri 635001, India
[c] Department of Physics, PSGR Krishnammal College for Women, Coimbatore 641004, India

ARTICLE INFO

Keywords:
Semiconductor
Nanoparticles
Cadmium sulfide
Nickel sulfide

ABSTRACT

The mixed phase CdS and NiS nanoparticles are prepared by adopting ultrasonic wave irradiation method under different doping concentration of Ni in CdS. The well defined nano spheres are obtained during this synthesis process. The predicted particle sizes from X-ray diffraction (XRD) analysis are found to lie in the range between 37 and 49 nm. The effective doping of Ni lead to form the mixture of two phases such as CdS and NiS. The respective change due to the formation of mixture of CdS and NiS is reflected well in the band gap energy which is measured in Diffused Reflectance Spectra (DRS). It is predicted in the range of 2.41–2.23 eV respectively. Consistency of particle size with XRD are confirmed from Transmission Electron Microscope (TEM) images and also identified the presence of Nickel Sulfide and Cadmium Sulfide in nanostate with average particle size as 54 nm. The Energy Dispersive X-ray (EDAX) analysis confirmed the existence of Ni, Cd and S the doping levels. The optical absorption analysis of samples are performed in UV–vis range 400–600 nm. The synthesized samples are further characterized Fourier Transform Infrared (FT-IR) spectroscopy, Thermogravimetric (TGA) analysis, I-V characteristic and conductivity measurements.

1. Introduction

The direct band gap material of CdS as 2.4 eV [1] at room temperature is the welcoming advantage in semiconductor. Now-a-days semiconducting sulfides are extensively used in different applications due to optoelectronic properties. This property can be highlighted only with the band gap energy of the material. In such a way, the CdS plays a crucial part in different useful applications like Photo luminescent devices, magnetic storage devices, photo detectors, chemical sensors, light emitting diodes, logic gates and electron transistors [2–7], optical and electrical properties [8], and photo catalytic devices [9].

The doping of transition metal in semiconductor is developed the interest towards wide variety of semiconductor device fabrication. Also it paves a path to derive optical and electrical properties in a single material. There are different doping elements like Mn, In, Ag and Co [10–13] which have been doped in CdS by many researchers. Recently, the Ni doped CdS nanoparticles have been prepared by following different routes such as dry process, chemical precipitation method [14], hydrothermal method [15], co-precipitation method [16]. Among these processes of preparation, the ultrasonic irradiation method is adopted in this work synthesis. An investigation is made on different doping weight percentage of Ni in CdS nanoparticles. The enhancement of band gab energy is also found due to doping of Ni. The percentage of doping of Ni in CdS is highly influenced on changing particles size. The electrical property analysis Ni doped CdS nanoparticles are also provided the applicable change in conductivity.

2. Experimental procedures

The chemicals used for the preparation were of analytical grade Cadmium Acetate Dehydrate [$Cd(CH_3COO)_2{\cdot}2H_2O$], Nickel Acetate Tetrahydrate [$Ni(CH_3COO)_2{\cdot}4H_2O$] and Sodium sulfide monohydrate [$Na_2S{\cdot}H_2O$], Sodium Hydroxide [NaOH].

2.1. Synthesis of CdS nanopowder

The synthesis of CdS nanopowder sample was prepared by ultrasonic wave irradiation method. A 100 ml aqueous solution was prepared by using 0.2 M solution of Cadmium Acetate and 0.1 M solution of Sodium Sulfide. The prepared solution was mixed and stirred for three hours at room temperature. The pH value was maintained as 8 during the reaction by using NaOH solution. Then,

* Corresponding author.
E-mail address: jprakash_jpr@rediffmail.com (R. Jayaprakash).

http://dx.doi.org/10.1016/j.mssp.2016.08.014
Received 2 June 2016; Received in revised form 26 July 2016; Accepted 18 August 2016
Available online 04 October 2016

the mixture of solution was allowed to irradiate in ultrasonic waves of frequency 39 kHz using sonication bath (ultrasonic bath model-PCi Analytics 100 H, 3.5 L capacity). The solution was sonicated for 3 h. Finally, the solution was filtered and dried for 15 h at 100 °C to remove the water content as well as easily evaporated by products. The resultant product was again annealed at 400 °C and named as sample (a). This sample was considered as a CdS nanopowder.

2.2. Synthesis of Ni Doped CdS nanopowder and NiS_2 nanopowder

The synthesis of nanocrystalline Ni doped CdS nanopowder sample was prepared by the same method. A 0.2 M solution of Cadmium Acetate and 0.1 M solution of Sodium Sulfide. The doping levels is varied by changing the weight ratio [Cd/Ni], in the solution as 10%, 20%, 30%, 40% and 50%. The solvent has been added to the solution and the mixture was stirred well for 3 h. The above solution was neutralized by adding of NaOH solution and pH of the solution was maintained as 8 by diluting with deionised water. Then, the mixture of solution was allowed to irradiate in ultrasonic waves of frequency 39 kHz using sonication bath (ultrasonic bath model-PCi Analytics 100 H, 3.5 L capacity). The solution was sonicated for 3 h. Finally the solution was filtered and dried at 100 °C by oven. The dried powders were sintered at higher temperature of 400 °C and named as sample (b)–(f) to obtain mixture of Ni doped CdS nanopowder. Similar procedure is adopted for synthesizing NiS nanoparticles and sintered this sample at 400 °C. This sample is named as sample (g).

2.3. Formation of CdO nanopowder

A small quantity of CdS nanopowder prepared under the above mentioned procedure in Section 2.1 is further heated to 900 °C for 1 h. Then the sample is cooled to room temperature. A phase transition is occurred from CdS to CdO at this temperature. This sample is considered as CdO nanoparticles and named as sample (h).

2.4. Characterization

The structure of the sample was analyzed by X-ray diffraction (XRD) using Rigaku X-ray diffraction unit model ULTIMA III. The morphology and size of the products were observed by High Resolution Transmission Electron Microscopy (HRTEM) and Selected Area Electron Diffraction (SAED) was recorded for the sample on a Technai G20-stwin using an accelerating voltage of 200 kV. The atomic percentage of Ni doped CdS powder was measured by using Energy Dispersive X-ray analysis (EDAX) by using JOEL 5600LV microscope at an accelerating voltage of 10 kV. The Thermal Analysis (TGA) of the sample was analyzed by using HITACHI TG/DTA 7300 in Nitrogen gas atmosphere. The property of conductivity was predicted by using Keithley 6517B Electrometer. The pure and Ni doped CdS was also characterized by Fourier Transform Infrared (FT-IR) spectra and the spectrum was recorded by using a 5DX FT-IR spectrometer. Ultraviolet (UV–visible DRS) absorption spectrum was also recorded by using JASCO V-670 Spectrophotometer.

3. Results and discussion

3.1. XRD analysis

Fig. 1(A)(a) is the X-ray diffraction pattern of undoped CdS nanopowder which shows the formation of cassiterite CdS structure. Fig. 1(A)(b)–(f) shows the XRD pattern of different wt% of Nickel doped with CdS nanopowder such as 10%, 20%, 30%, 40% and 50% respectively and heated at 400 °C. The peaks in Fig. 1(a) can be identified as the (100), (002), (101), (102), (110), (103), (112), (002), (203), (210), (211), (114) and (105) for CdS nanoparticles (PDF JCPDS No. 80-0006) for sample (a) which belongs to hexagonal phase [17].

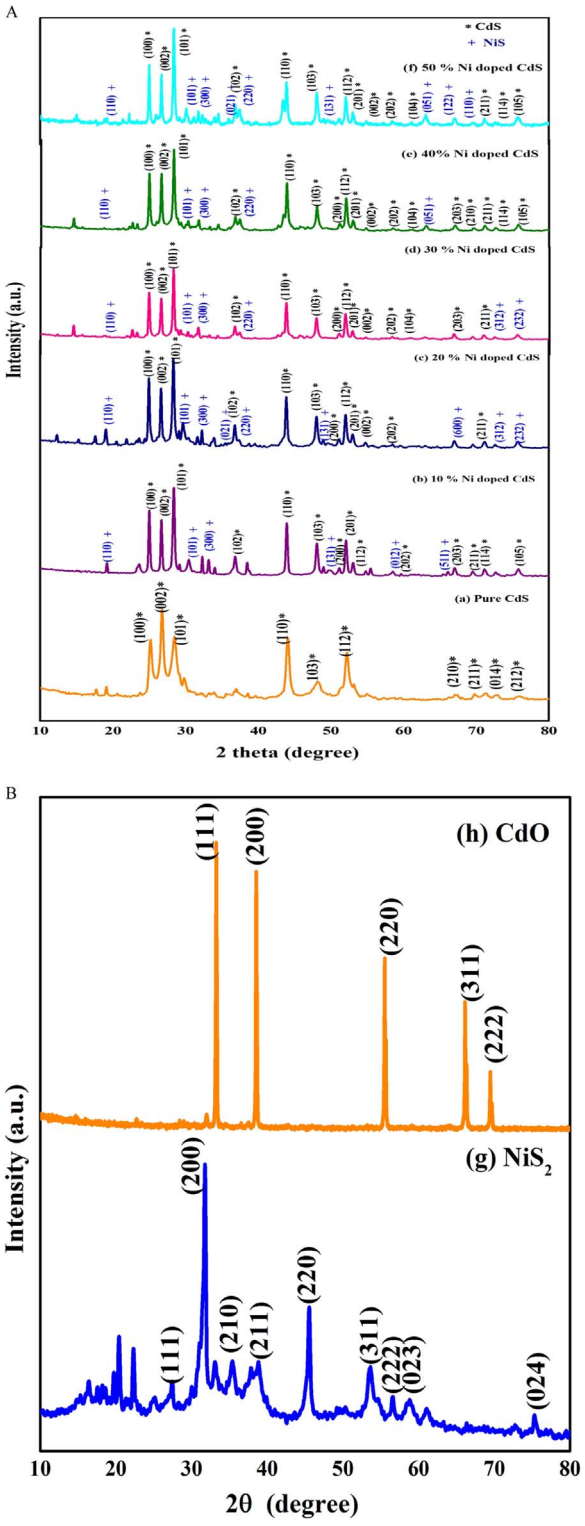

Fig. 1. (A) XRD patterns of undoped CdS and Ni doped CdS nanoparticles. (B) XRD patterns of NiS_2 and CdO nanoparticles.

The calculated unit cell parameters for CdS nanoparticles are a=4.121 Å and C=6.682 Å.

Fig. 1(A)(b)–(f) shows the diffraction pattern of 10 wt%, 20 wt%, 30 wt%, 40 wt%, and 50 wt% of Ni doped with CdS and named as sample b, c, d, e and f respectively. These XRD patterns are confirmed the crystallinity and mixed phase according to the doping percentage. As expected the peaks obtained for undoped CdS significantly changed due to the doping of Ni in CdS. The miller indices belong to the sample

b from diffraction pattern as (100), (002), (101), (102), (110), (103), (200), (201), (112), (202), (203), (211), (114) and (105) respectively. All these referred peaks are well matched towards the phase of CdS with hexagonal phase (# JCPDS No. 80-0006). At the same time other peaks possessed the miller indices such as (110), (101), (300), (131), (012) and (511). These peaks are well matched for NiS nanopowder with rhombohedral phase (# JCPDS No. 65-2117). The change can be occurred due to the replacement of Cd^{2+} by Ni^{2+} at different lattice site of CdS [8]. As well as there is no appreciable shift in corresponding XRD peaks belong to undoped CdS due to doping of Ni. Apart from this there are additional peaks obtained for NiS. The confirmation peaks for the crystallinity reveals that the number of peaks belongs to NiS is lesser than the peaks belongs to CdS sulfide for the sample (b).

Fig. 1(A)(c) shows the diffraction pattern of 20 wt% Ni doped CdS. It confirms that the sample shows the presence of both NiS and CdS crystalline phase. The respective diffraction peaks at (100), (002), (101), (102), (110), (103), (200), (201), (112), (002), (202) and (211) are matched for CdS with hexagonal phase (# JCPDS No. 80-0006). Similarly, the miller indices of the peaks such as (110), (101), (300), (021), (220), (131), (012), (051), (600), (312) and (232) are matched for NiS with rhombohedral phase (# JCPDS No. 65-2117). On comparison with the presence of number peaks of NiS and CdS confirmed that almost equal number of peaks of CdS and NiS are presented in the XRD pattern of this sample.

Fig. 1(A)(d)–(f) are represented diffraction pattern of 30 wt%, 40 wt% and 50 wt% of Ni doped CdS nanopowder. The diffraction peaks of (100), (002), (101), (102), (110), (103), (200), (201), (112), (002), (202) and (211) are matched for CdS nanopowder hexagonal phase (# JCPDS No. 80-0006) for all different doping levels. Similarly, the 7 respective peaks of such as (110), (101), (220), (051), (511), (312) and (232) belong to 30 wt% of Ni doping level and (101), (300), (220) and (051) *hkl* values of 4 peaks belong to 40 wt% of Ni doping levels. Finally there are 9 peaks which obtained for 50 wt% of Ni doping level such as (110), (101), (300), (021), (131), (051), (122), and (110).

Fig. 1(B)(g) represented diffraction pattern of NiS_2 nanopowder. The Diffraction peaks of (111), (200), (210), (211), (220), (311), (222), (023) and (024) are matched for NiS_2 nanopowder with cubic phase (#JCPDS No. 65-3325). Similarly, the recorded XRD pattern of heated CdS nanoparticles further up to 900 °C possesses the diffraction peaks such as (111), (200), (220), (311) and (222). These peaks are well matched towards corresponding cubic phase. (#JCPDS No. 65-2908). These peaks confirm that the occurrence of phase transition from CdS to CdO is observed while heating the sample at 900 °C.

The crystalline size of the nanoparticles were calculated by using the Debye-Scherrer's formula,

$$D = \frac{0.9\lambda}{\beta \cos\theta}$$

where D is the Grain Size, K is a constant of value 0.94, λ is the wavelength of the X ray radiation (1.5 Å), and β is the full width half maximum and θ is the angle of diffraction. The average particle size is predicated by the Debye-Scherrer's formula as 27 nm for annealed sample at 400 °C. Similarly the average particle size of Ni doped CdS nanoparticles is predicted as 37 nm for 10% Ni doped CdS, 37 nm for 20% Ni doped CdS, 41 nm for 30% Ni doped CdS, 47 nm for 40% Ni doped CdS, and 49 nm for 50% Ni doped CdS. The average particle size is calculated for NiS_2 nanoparticles as 61 nm. Similarly, the average particle size of CdO nanoparticles are predicted for sample (h) as 98 nm. The larger particle size of CdO after heating is also revealed that the increase in temperature is influenced more for increasing the particle size.

These results reveal that 10 wt% Ni and 20 wt% Ni doped CdS nanoparticles posses almost same particle size, 20 wt% and 50 wt% of Ni doped CdS nanopowder are having equal number of CdS and NiS peaks. But Ni doped CdS nanopowder of 20 wt% possesses less particle size than the 50 wt% of Ni doped CdS nanopowder. These results from

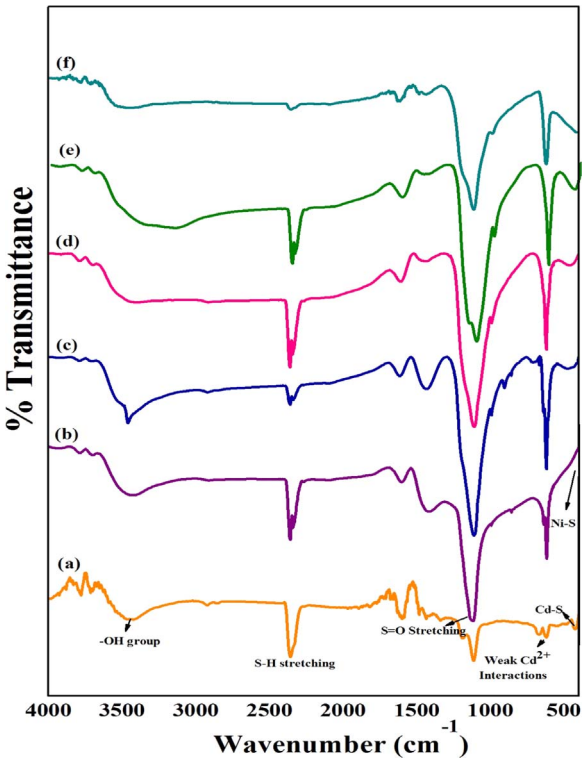

Fig. 2. FT-IR spectrum of undoped CdS and Ni doped CdS nanoparticles.

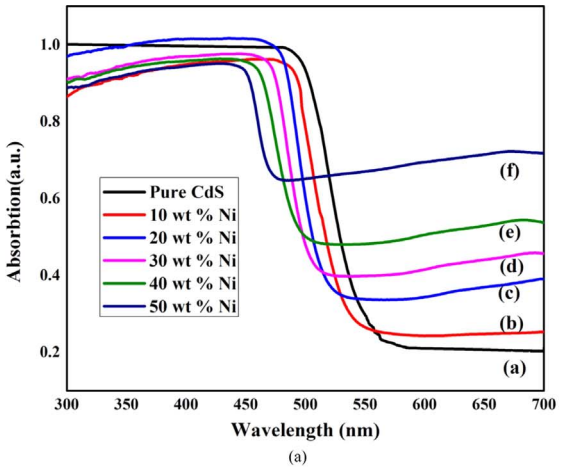

Fig. 3. A (a–f) UV–vis absorption spectra for undoped CdS and Ni doped CdS nanoparticles. B (a–f) Band gap evaluation for undoped and Ni doped CdS nanoparticles.

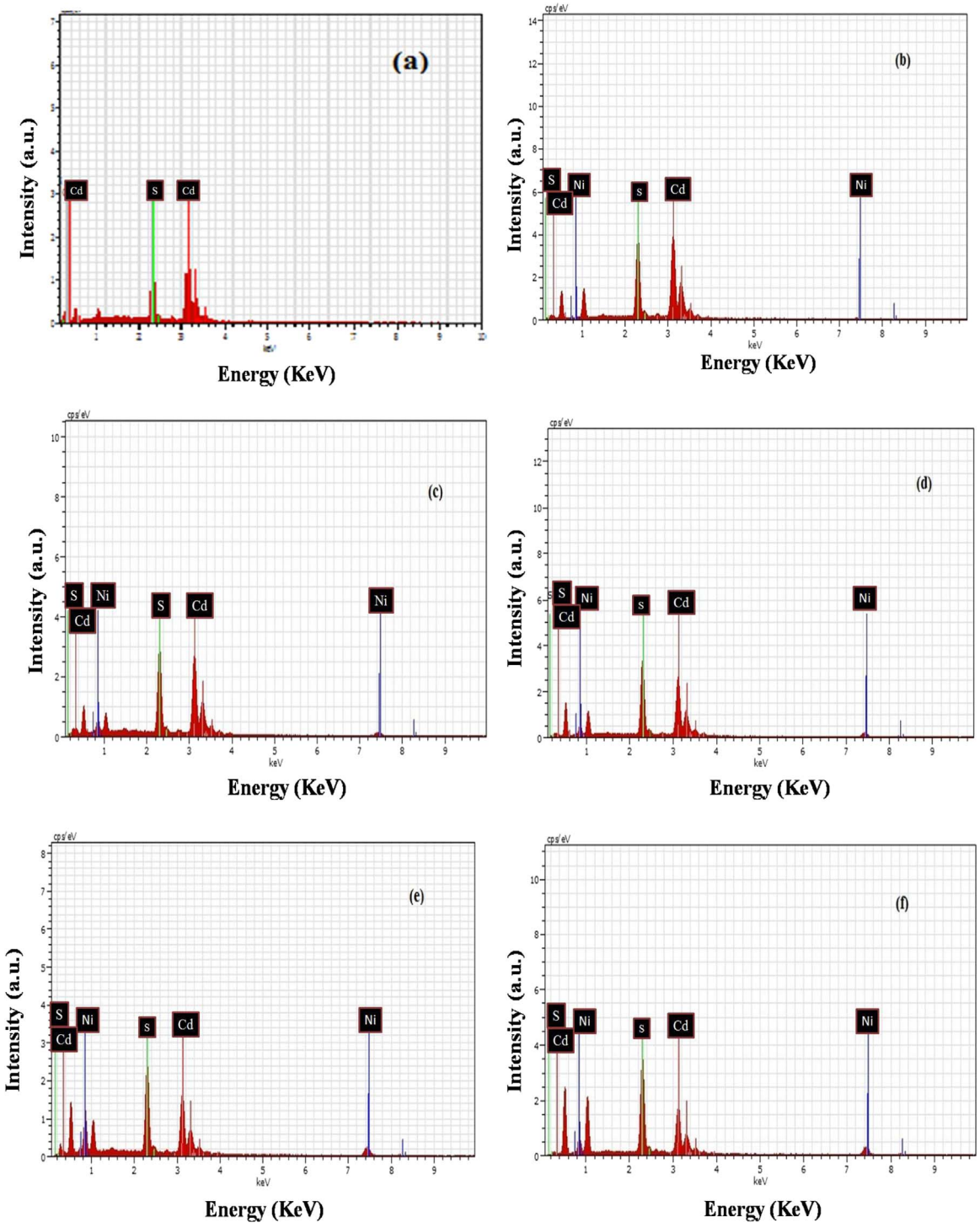

Fig. 4. EDAX spectra of the undoped and Ni doped CdS nanoparticles.

Table 1
wt% and at% of undoped and Ni doped CdS nanoparticles.

Samples	wt%			at%		
	Cd	S	Ni	Cd	S	Ni
Pure CdS	79.17	20.83	–	52.02	47.98	–
10 wt% of Ni	81.48	18.26	0.27	55.81	43.84	0.34
20 wt% of Ni	75.66	20.01	4.34	49.10	45.51	5.39
30 wt% of Ni	72.77	22.58	4.65	45.25	49.22	5.54
40 wt% of Ni	61.83	31.02	7.15	33.55	59.02	7.43
50 wt% of Ni	66.89	17.18	15.93	42.43	38.21	19.36

the XRD pattern reveal that the reaction of Nickel plays a dominant role in reacting with cadmium sulfide and forms a mixture of NiS phase and CdS phase and becomes a composite [18]. Thus 20 wt% of Ni doping level is confirmed as the best from the analysis due to the formation of lesser particles size than the other doping levels.

The XRD pattern is recorded for NiS_2 nanoparticles the pattern belongs to this sample (g) is cubic phase. Also from the analysis, the CdS possesses hexagonal phase but NiS_2 nanoparticles comes under the category of cubic phase. The equal number of peaks of CdS and NiS are appeared after doping of Ni doped CdS. The phase belongs to CdS is hexagonal and NiS becomes rhombohedral phase only due to doping of

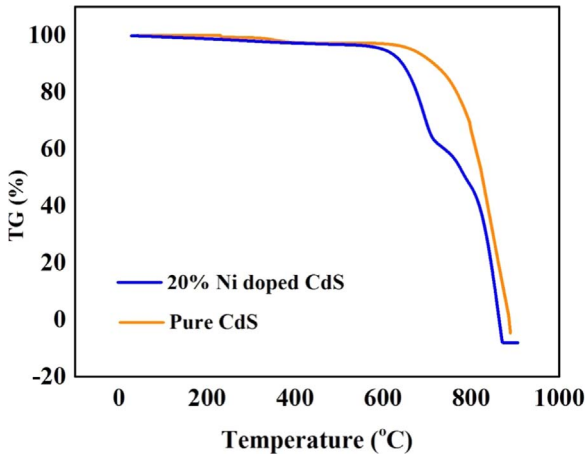

Fig. 5. TG Analysis of undoped CdS and 20 wt% of Ni doped CdS nanoparticles.

Ni in CdS. So this formation of NiS is considered as secondary phase [18]. Because the NiS_2 alone possesses cubic phase and the obtained corresponding peaks of NiS in Ni doped CdS stage is changed into rhombohedral phase. It reveals that NiS and CdS becomes a mixture. The reason for this is due to miss match of phase between NiS and CdS. This result is confirmed as mixture of CdS and NiS not a composite.

3.2. FT–IR spectrum analysis

FT–IR spectra of samples (a)–(f) were also recorded and are shown in Fig. 2(a)–(f). Fig. 2(a) represents FT–IR pattern for undoped CdS nanoparticles. Fig. 2(b)–(f) represent FT-IR spectra of Ni doped CdS nanopowder. The assigned peaks at 3699 cm^{-1} and 3790 cm^{-1} in Fig. 2(a), the peaks 3432 cm^{-1} and 3790 in Fig. 2(b), the peaks around at 3460 cm^{-1} and 3791 cm^{-1} in Fig. 2(c), the peaks 3156 cm^{-1} and 3789 cm^{-1} in Fig. 2(d), the peaks 3458 cm^{-1} and 3793 cm^{-1} in Fig. 2(e), and the peaks around at 3403 cm^{-1} and 3789 cm^{-1} in Fig. 2(f) are identified the characteristic absorption of –OH group [19]. Similarly, the absorption peaks at 1111 cm^{-1} in Fig. 2(a), 1118 cm^{-1} in Fig. 2(b), 1111 cm^{-1} in Fig. 2(c), 1108 cm^{-1} in Fig. 2(d), 1108 cm^{-1} in Fig. 2(e), 1108 cm^{-1} in Fig. 2(f) of the all samples (a–f) are represented the vibration of S=O stretch [20]. The absorption peaks at 2360 cm^{-1} in Fig. 2(a), 2359 cm^{-1} in Fig. 2(b), 2358 cm^{-1} in Fig. 2(c), 2342 cm^{-1} in Fig. 2(d), 2342 cm^{-1} in Fig. 2(e), 2359 cm^{-1} in Fig. 2(f) are attributed to S-H stretching vibrations [21]. The weak vibrations absorption peak lies at 428 cm^{-1} is belonged to the metallic presence of Cd-S in Fig. 2(a) [22]. Similarly, the significant peaks at 618 cm^{-1} in all the samples are also identified the metallic presence Cd-S, Ni-S and weak Cd^{2+} interactions in all the doping levels [18].

3.3. UV–visible DRS absorption spectra

Fig. 3(A) is absorption spectra of undoped CdS and Ni doped CdS at different concentration. The absorption edge for undoped CdS is 572 nm. The absorption edge observed for 10 wt% Ni doped CdS nanoparticles 538 nm. Similarly, the respective absorption edge is obtained during this study as 523 nm for 20 wt% Ni doped CdS, and 515 nm for 30 wt% Ni doped CdS, and 507 nm for 40 wt% Ni doped CdS, and 493 nm for 50 wt% Ni doped CdS. The optical absorption measurement shows the absorption edge of undoped CdS move towards shorter wavelength at high percentage of Ni doping in CdS. The absorption edge shift towards the blue region in the UV–vis spectrum. This shift also confirms the increasing the particle size due to increasing doping levels. This increasing particle size is also evidenced in the XRD pattern. The optical band gap variation is also observed from this study during the band gab calculation. The optical band gap is determined from UV–visible DRS absorption spectra of pure and Ni doped CdS nanoparticles. The band gap energy is predicted as 2.413 eV for the sample (a) 2.374 eV for sample (b), 2.329 eV for the sample (c), 2.299 eV for the sample (d), 2.270 eV for the sample (d) 2.241 eV for the sample (d) shown in Fig. 3(B). The plots of $(\alpha h\nu)^2$ versus energy ($h\nu$) for different undoped CdS and Ni doped CdS of samples (a)–(f) are shown in Fig. 3(B). It concludes that doping concentration of Ni from 10% to 50% decreases the band gap energy from 2.413 to 2.241 eV. The decrease in band gap energy due to the increase of NiS formation as observed from the XRD which influenced more for decreasing band gap energy. Particle size is also increased due to doping level of Ni in CdS which can strongly lead to decrease in band gap energy [23]. So the particle size is the significant factor which creates change in band gap in CdS doped Ni nanoparticles. The rate of increase in doping concentration creates a change in particle size. Elango et al., also reported that the particle size variation has changed the optical property of the material [18]. The optical property change is highly influenced for different doping level of Ni in CdS nanoparticles. Due to this reason the obtained (Eg) energy gap values are decreased for the Ni doped CdS than undoped CdS.

3.4. Energy dispersive analysis of X-ray (EDAX)

Fig. 4(a)–(f) shows the EDAX spectra of pure and Ni doped CdS (10%, 20%, 30%, 40%, 50%) nanoparticles which clearly reflect the absentia of other impurities and contaminations in the samples. Table 1 provides the elemental composition in terms of atomic percentage and weight percentage obtained from EDAX spectra for all samples indicating the presence of Cd:S:Ni.

The EDAX spectrum is recorded at five different weight percentage levels on each sample to ascertain the homogeneity of the Ni incorporation in the CdS nanoparticles. It reveals that Cd, Ni and S elements are present in the samples and the ratio of the atomic percentage of the elements in the samples matches stoichiometric of with the quantity taken for their preparation. The prepared CdS and Ni doped CdS are found to be as no contamination.

3.5. Thermogravimetric analysis

The thermal behavior of dried Ni doped CdS nanoparticles are investigated for undoped CdS and Ni doped CdS by TG-DTA. The decomposition behavior is recorded under different temperature as shown in Fig. 5(a) and (b). The both samples are tested in a nitrogen atmosphere. The decomposition of the CdS started in the nitrogen atmosphere at above 700 °C. When the temperature is increased, the hexagonal phase of CdS nanoparticles is disappeared and CdO phase is formed due to increase of temperature and a further decomposition occurs upto1100 °C [24]. Also it confirms that the absorption of oxygen creates the mass variation during decomposition. In this stage the rapid decomposition of CdS is stimulated towards occurrence of CdO phase. The sample (a) is heated to 900 °C and confirmed the phase change of CdS into CdO by XRD pattern which is shown in Fig. 1(B)(h). It depicts that the CdS nanoparticles with hexagonal phase is fully changed and it becomes CdO nanoparticles with cubic phase. A small hump at 12.0% decomposition level and 74.6% decomposition level reveals the prominent change in phases. It confirms well that more oxygen is replaced the position of sulfur.

Similarly, the temperature was increased in Ni doped CdS nano-powder sample, this process reveals that the NiS nanoparticles is disappeared and formed into NiO at 300 °C to 400 °C range. It is well identified from the in Fig. 5(b). The small hump is shown in the 300 °C to 350 °C temperature range. The 1% weight loss is observed when the temperature reached at 300 °C. The weight loss is calculated for this sample as 26.4% in nitrogen atmosphere at 800 °C.

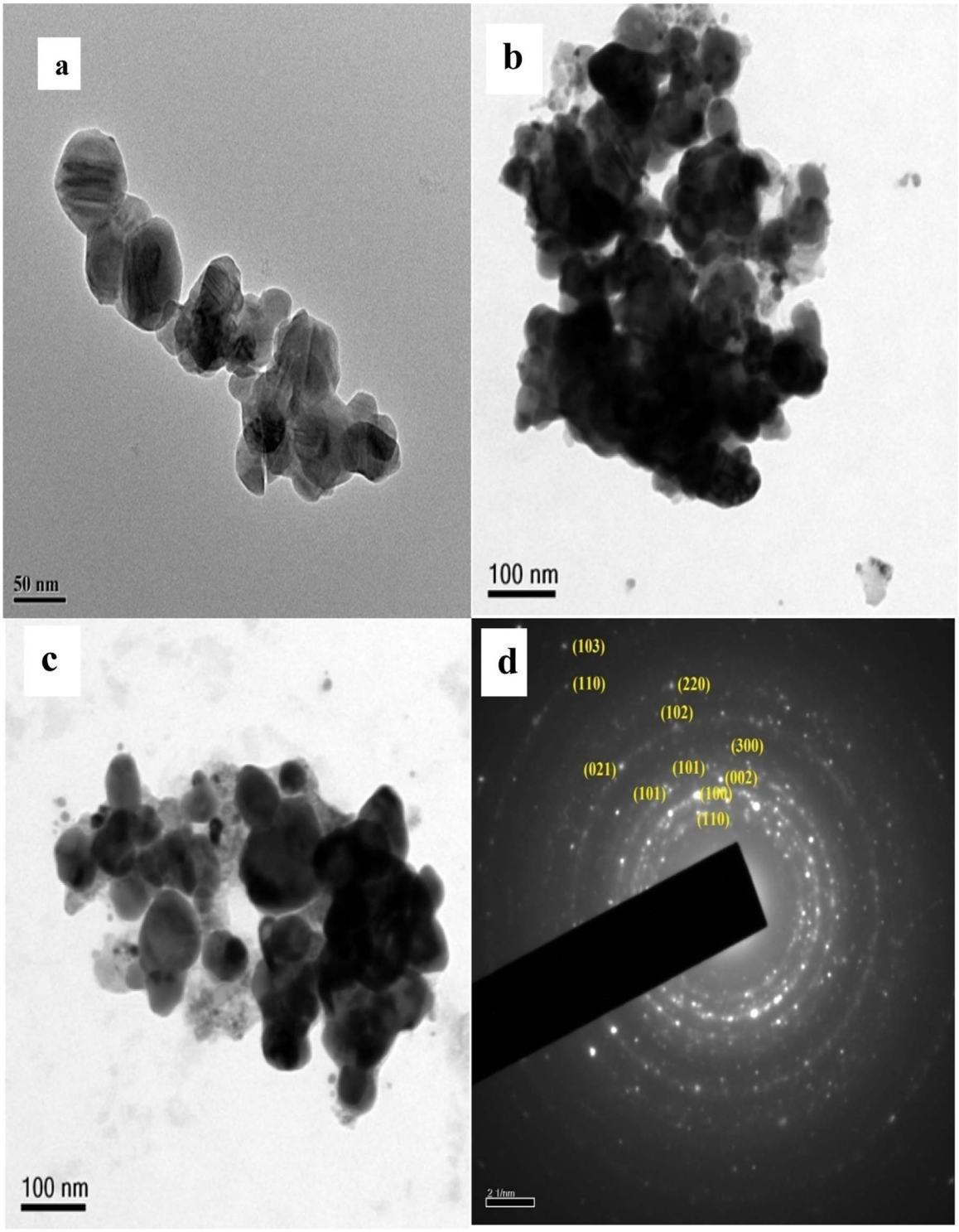

Fig. 6. (a) TEM micrograph of undoped CdS nanoparticles (b, c) Ni doped CdS nanoparticles (d) SAED pattern of Ni doped CdS nanoparticles.

3.6. Transmission electron microscope

TEM images of the pure and Ni doped CdS nanoparticles are shown in Fig. 6(a)–(c). The spherical shape is observed and they are in agglomerated state of size ranging from 60 to 64 nm for undoped CdS nanoparticles. The image of the Ni doped CdS nanopowder is clearly visualized the spherical shaped particles with particle size 54 nm are observed from this Fig. 6(c). The increase in the size and change in shape are observed due to the addition of Ni as dopant. The perfectness of the spherical shape of the nanoparticles is observed from the TEM images for the Ni doped samples than the undoped CdS samples.

The pictures b and c also indicate the dark spherical shaped particles among with smaller bright particles. On comparison with the picture (a) undoped CdS samples become brighter than the Ni doped CdS. Because this undoped CdS are more transparent than Ni doped CdS. Thus the appearance of bright and darkness of spherical particles in these pictures also reveal the presence of well separated NiS and CdS nanoparticles as observed in the XRD pattern. The NiS particle presence in the picture b and c creates less transparent spherical shaped particles. This can also be seen from the variation

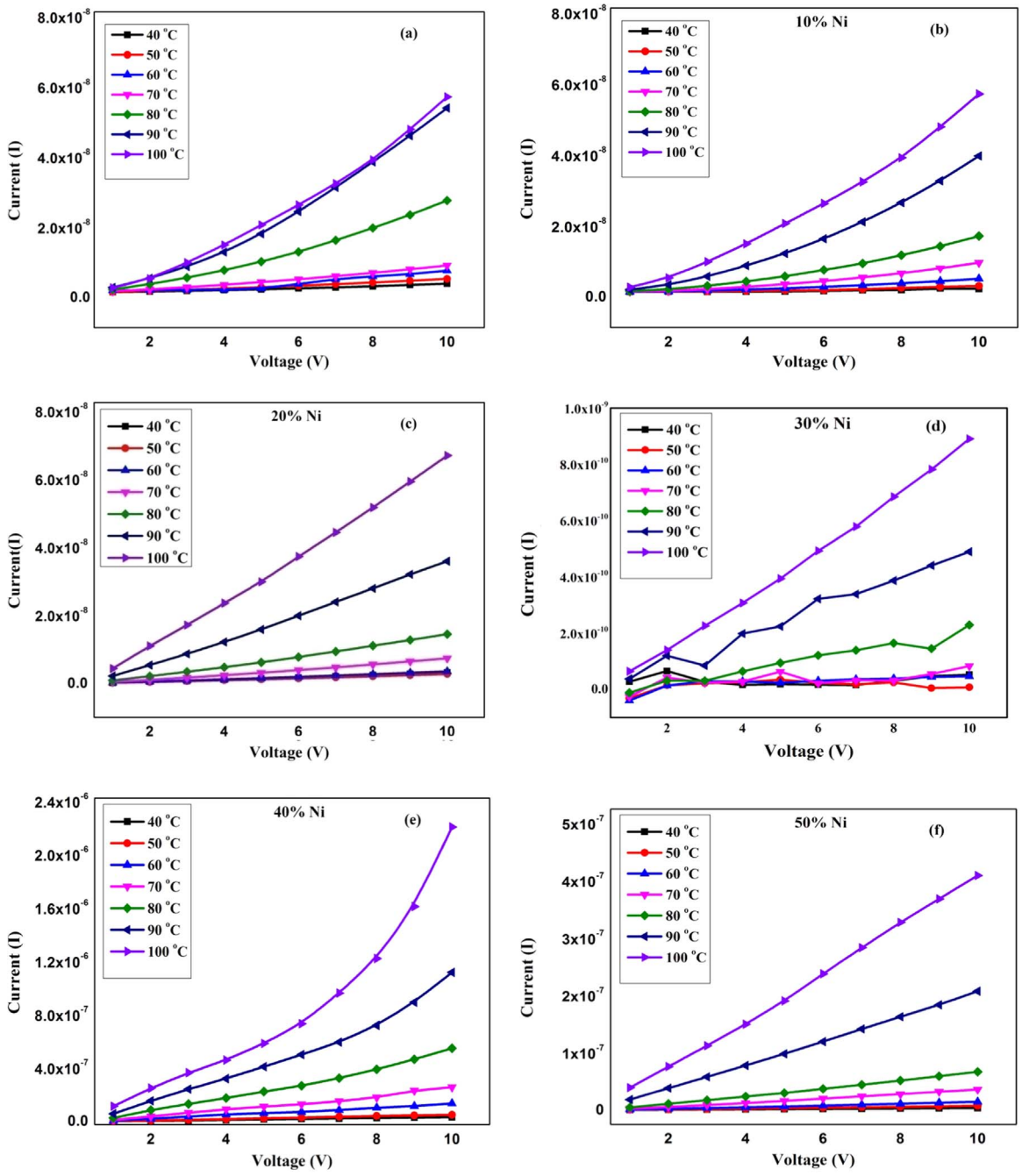

Fig. 7. (a–f) I-V characterization of undoped CdS and Ni doped CdS nanoparticles.

of band gap due to the formation of mixed nature of NiS nanoparticles in CdS nanoparticles. Fig. 6(d) shows selected area electron diffraction (SAED) pattern which indicates that the Ni doped CdS nanoparticles are polycrystalline in nature. The diffraction planes of the corresponding main peaks as observed in the XRD are well matched with the concentric circles of the SAED pattern.

3.7. Electrical properties

The electrical conductivity of Ni doped CdS nanoparticles are measured at different temperatures. Fig. 7(a)–(f) shows typical current (I) versus voltage (V) characteristic of synthesized pure and Ni doped CdS nanoparticles. It exhibits a nearly linear response to the applied voltage for different temperatures. This linear response due to voltage variation shows semiconductor behavior. Fig. 8(a)–(f) represent the variation of conductivity with respect to temperature for different voltages such as 2 V, 4 V, 6 V, 8 V and 10 V respectively. Fig. 8(a) shows that conductivity at high temperature at 2 V shows the 23.26 S cm^{-1} therefore, it is found that there is decrease in conductivity as 19.68 S cm^{-1} at that respective voltage for decrease of temperature. Also the similar response is observed as 23.00 S cm^{-1} to 19.76 S cm^{-1} for 4 V, 22.79 S cm^{-1} to 19.70 S cm^{-1} for 6 V, 22.65 S cm^{-1} to 19.47 S cm^{-1} for 8 V, 22.56 S cm^{-1} to 19.11 S cm^{-1} for 10 V in undoped CdS nanoparticles.

The conductivity response for 10 wt% Ni doped CdS is shown in Fig. 8(b). The conductivity at high temperature at 2 V is 25.86 S cm^{-1} and 19.68 S cm^{-1} for low temperature. Similarly, the conductivity variation with respect to temperature is observed as 24.58 S cm^{-1} to 19.76 S cm^{-1} for 4 V, 24.42 S cm^{-1} to 19.70 S cm^{-1} for 6 V, 24.81 S cm^{-1} to 19.47 S cm^{-1} for 8 V, 24.24 S cm^{-1} to 19.11 S cm^{-1}

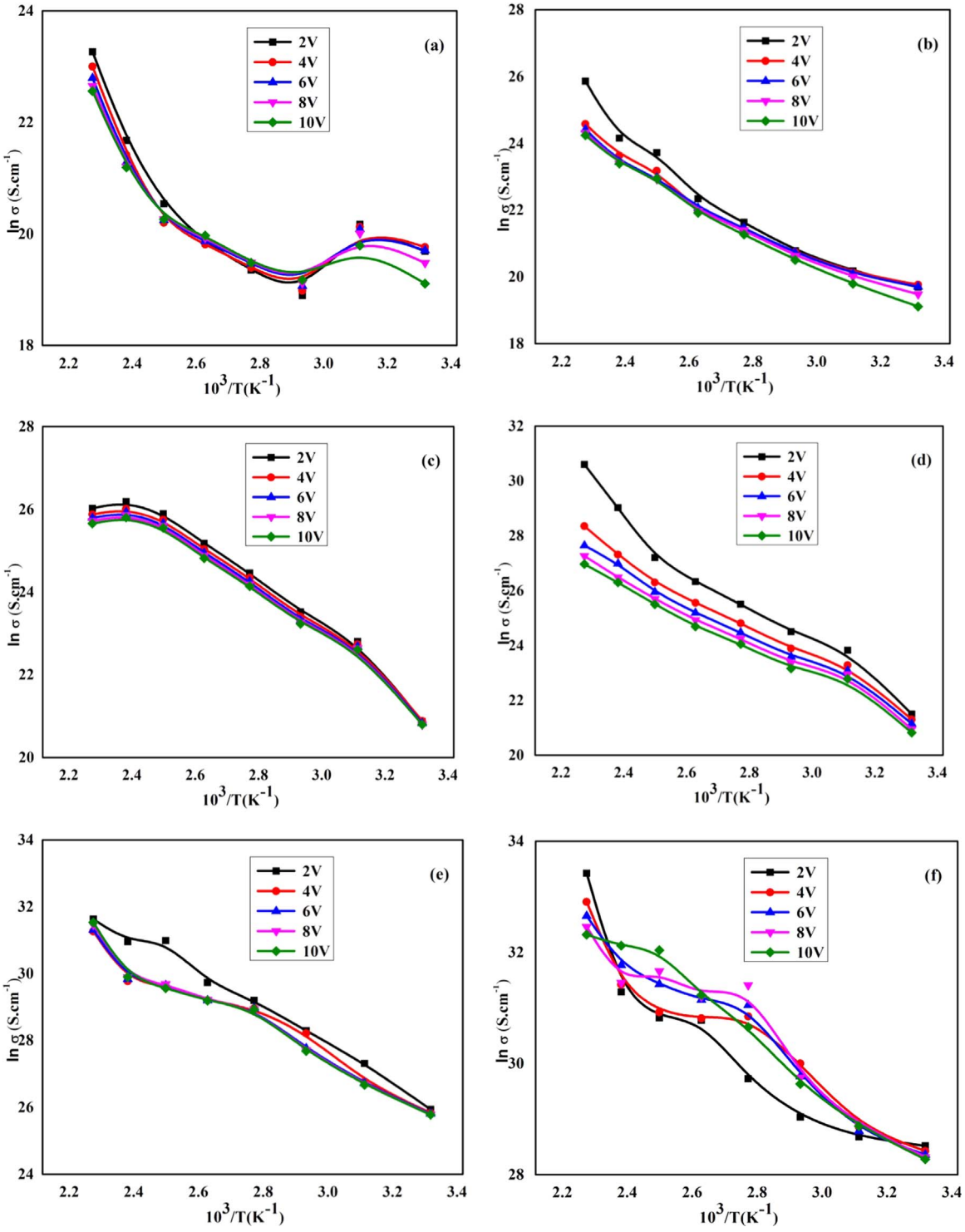

Fig. 8. (a–f) Conductivity as function of temperature for undoped and Ni doped CdS nanoparticles.

for 10 V. The conductivity changes are recorded for 20 wt% Ni doped CdS, 30 wt% Ni doped CdS, 40 wt% Ni doped CdS, and 50 wt% Ni doped CdS are shown Fig. 8(c)–(f). The similar trend is observed in all the doping levels for variation of temperature with respect to conductivity variation as 26.02 S cm^{-1} to 20.86 S cm^{-1} for 2 V, 25.87 S cm^{-1} to 20.88 S cm^{-1} for 4 V, 25.79 S cm^{-1} to 20.82 S cm^{-1} for 6 V, 25.71 S cm^{-1} to 20.79 S cm^{-1} for 8 V, 25.65 S cm^{-1} to 20.79 S cm^{-1} for 10 V in 20 wt% doping level of CdS nanoparticles, 30.59 S cm^{-1} to 21.49 S cm^{-1} for 2 V, 28.35 S cm^{-1} to 21.29 S cm^{-1} for 4 V, 27.64 to 21.14 for 6 V, 27.26 S cm^{-1} to 20.94 S cm^{-1} for 8 V, 26.96 S cm^{-1} to 20.81 S cm^{-1} for 10 V in 30 wt% doping level of CdS nanoparticles, 31.63 S cm^{-1} to 25.93 for 2 V, 31.26 S cm^{-1} to 25.83 S cm^{-1} for 4 V, 31.30 S cm^{-1} to 25.80 S cm^{-1} for 6 V, 31.46 S cm^{-1} to 25.78 S cm^{-1} for 8 V, 31.52 S cm^{-1} to 25.78 S cm^{-1} for 10 V in 40 wt% doping level of CdS nanoparticles, 33.42 S cm^{-1} to 28.51 S cm^{-1} for 2 V, 32.90 S cm^{-1} to 28.42 S cm^{-1} for 4 V, 32.65 S cm^{-1} to 28.35 S cm^{-1} for 6 V, 32.45 S cm^{-1} to 28.31 S cm^{-1} for 8 V, 32.32 S cm^{-1} to 28.27 S cm^{-1} for 10 V in 50 wt% doping level of CdS nanoparticles respectively.

The linear variation of conductivity with respect to temperature

shows that almost similar trend for 10 wt% Ni doping level of CdS and 20 wt% doping level of CdS. The reason for this behavior is due to less particles size and also the attainment of almost nearest particle size in 10 wt% and 20 wt% Ni doping levels in CdS. Further doping levels retain the similar behavior trend and reaches towards higher value of conductivity for the respective doping levels of 30 wt% of Ni, 40 wt% of Ni, and 50 wt% of Ni respectively. In overall analysis of conductivity variation for different doping levels of Ni in CdS confirmed that the electrical conductivity is found to be in the range of 19.11 S cm^{-1} to 23.26 S cm^{-1} for undoped CdS. The electrical conductivity measured is in the range between 19.12 S cm^{-1} to 33.42 S cm^{-1} for Ni doped CdS for different doping levels. The highest value of electrical conductivity may be due to the less particle size, as well as homogeneous distribution of grain in the cubic lattice and ionic mobility. It is well found that the Ni doping in CdS leads to carrier doping, which consequently decreases the energy gap and hence increases the conductivity.

4. Conclusion

The nanospheres of Ni doped CdS are synthesized by the Ultrasonic wave irradiation method. The XRD analysis confirmed that NiS as secondary phase possessed rhombohedral due to doping instead of NiS as cubic phase. The effect of doping Ni on the CdS nanoparticles is found by band gap energy variation of the samples by DRS spectra of respective wave length. The CdS with hexagonal phase and NiS with rhombohedral phase in spherical shaped morphology was formed in the presence of Ultrasonic irradiation due to different doping concentration. This study reveals that the best doping percentage of Ni in CdS with optimum particle size has been observed. The XRD analysis for 20 wt% of Ni CdS nanoparticles showed the good crystallinity with less particle size. The specific band gap energy can be tapped on doping of CdS will Ni in different concentration. Also this method supports to identify that the doping of Ni in CdS reduces the band gap energy and increases the conductivity.

References

[1] D.C. Onwudiwe, T. Arfin, C.A. Strydom, Synthesis, characterization, and dielectric properties of N-butyl aniline capped CdS nanoparticles, Electrochim. Acta 116 (2014) 217–223.

[2] N.M. Ushakov, G.Yu Yurkov, D.A. Branov, K.V. Zapsis, M.N. Zhuravleva, V.I. Kochubei, I.D. Kosobudskii, S.P. Gubin, Opt. Spectrosc. 101 (2006) 248–252.

[3] J.S. Kulkarni, O. Kazakova, J.D. Holmes, Dilute magnetic semiconductor nanowires, Appl. Phys. A 85 (2006) 277–286.

[4] M.A. Mahdi, J.J. Hassan, S.S. Ng, Z. Hassan, N.M. Ahmad, Synthesis and characterization of single-crystal CdS nanosheet for high-speed photodetection, Phys. E: Low-Dimens. Syst. Nanostruct. 44 (2012) 1716–1721.

[5] Ren-Min Ma, Lun Dai, Guo-Gang Qin, High-performance nano-schottky diodes and nano-MESFETs made on single CdS nanobelts, Nano Lett. 7 (2007) 868–873.

[6] X. Duan, Y. Huang, R. Agarwal, C.M. Lieber, Single-nanowire electrically driven lasers, Nature 421 (2003) 241–245.

[7] G.Z. Shen, J.H. Cho, J.K. Yoo, G.C. Yi, C.J. Lee, Synthesis of single-crystal CdS microbelts using a modified thermal evaporation method and their photoluminescence, J. Phys. Chem. B 109 (2005) 9294–9298.

[8] A. Rmili, F. Ouachtari, A. Bouaoud, A. Louardi, T. Chtouki, B. Elidrissi, H. Erguig, Structural, optical and electrical properties of Ni-doped CdS thin films prepared by spray pyrolysis, J. Alloy. Compd. 557 (2013) 53–59.

[9] D. Ayodhyal, M. Venkatesham, A.S. kumari, G. Bhagavanth Reddy, G. Veerabhadram, One-pot sonochemical synthesis of CdS nanoparticles: photocatalytic and electrical properties, Int J. Ind. Chem. 6 (2015) 261–271.

[10] M. Liu, Y. Du, L. Ma, D. Jing, L. Guo, Manganese doped cadmium sulfide nanocrystal for hydrogen production from water under visible light, Int J. Hydrog. Energy 37 (2012) 730–736.

[11] D.R. Acostaa, C.R. Magan, A.I. Mart!ıneza, A. Maldonado, Structural evolution and optical characterization of indium doped cadmium sulfide thin films obtained by spray pyrolysis for different substrate temperatures, Sol. Energy Mater. Sol. Cells 82 (2004) 11–20.

[12] Jun Ma, Guo'an Tai, Wanlin Guo, Ultrasound-assisted microwave preparation of Ag-doped CdS nanoparticles, Ultrason Sonochem. 17 (2010) 534–540.

[13] M. Thambidurai, N. Muthukumrasamy, Dhayalan Veauthapillai, S. Agilan, R. Balasundaraprabhu, Impedance spectroscopy and dielectric properties of cobalt doped CdS nanoparticles, Powder Technol. 217 (2012) 1–6.

[14] A. Mercy, A.J. Anandhi, K.S. Murugesan, R. Jayavel, R. Kanagadurai, B.M. Boaz, Synthesis, structural and property studies of Ni doped cadmium sulphide quantum dots stabilized in DETA matrix, J. Alloy. Compd. 593 (2014) 213 (210).

[15] S. Devi, P. Korake, S.N. Achary, N.M. Gupta, Genesis of enhanced photoactivity of CdS/Ni_x nanocomposites for visible-light-driven splitting of water, Int. J. Hydrog. Energy 39 (2014) 19424–19433.

[16] K.S. Kumar, A. Divya, P.S. Reddy, S. Uthanna, R. Martins, E. Elangovan, Structural and optical behaviour of Ni doped CdS nanoparticles synthesized by chemical Co-precipitation method, Acta Phys. Pol. A 120 (2011) A52–A54.

[17] S.V. Kahane, R. Sasikala, B. Vishwanadh, V. Sudarsan, S. Mahamuni, CdO-CdS nanocomposites with enhanced photocatalytic for hydrogen generation from water, Int. J. Hydrog. Energy 38 (2013) 15012–15018.

[18] M. Elango, D. Nataraj, K.P. Nazeer, M. Thamilselvan, Synthesis and characterization of nickel doped cadmium sulfide ($CdS:Ni^{2+}$) nanoparticles, Mater. Res. Bull. 47 (2012) 1533–1538.

[19] Y. Zhao, H. Liu, F. Wang, J. Liu, K.C. Park, M. Endo, A simple route to synthesize carbon-nanotube/cadmium-sulfide hybrid heterostructures and their optical properties, J. Solid State Chem. 182 (2009) 875–880.

[20] H. Gunzler, H.U. Gremlich, Infrared Spectroscopy an Introduction, Wiley – VCH, Weinheim, Germany, 2002.

[21] R. Silverstin, F. Webster, Spectrometric Identification of Organic Compounds, College of Environmental Science & Forestry, New York, 2013.

[22] T.D. Kose, S.P. Ramteke, Studies on synthesis and electrical properties of CdS-polyaniline nanocomposite via oxidation polymerization, Int J. Comp. Mater. 2 (4) (2012) 44–47.

[23] M. Thambdurai, N. Muthukumarasamy, S. Agilan, N.S. Arul, N. Murugan, R. Balasundaraprabhu, Structural and optical characterization of Ni-doped CdS quantum dots, J. Mater. Sci. 46 (2011) 3200–3206.

[24] M. Kristl, Irena Ban, A. Danc, V. Danc, M. Drofenik, A sonochemical method for the preparation of Cadmium sulfide and cadmium selenide nanoparticles in aqueous solution, Ultrason. Sonochem. 17 (2010) 916–922.